Atmos. Chem. Phys. Discuss., doi:10.5194/acp-2016-995, 2016
Manuscript under review for journal Atmos. Chem. Phys.
Published: 17 November 2016

Atmospheric Chemistry and Physics Discussions

Heterogeneous uptake of ammonia and dimethylamine into sulfuric and oxalic acid particles

Meike Sauerwein[1] and Chak Keung Chan[1,2,3]

[1]Division of Environment, Hong Kong University of Science and Technology, Clear Water Bay, Kowloon, Hong Kong
[2]Department of Chemical and Biomolecular Engineering, Hong Kong University of Science and Technology, Clear Water Bay, Kowloon, Hong Kong
[3]School of Energy and Environment, City University of Hong Kong, Kowloon, Hong Kong

Correspondence to: Chak Keung Chan (Chak.K.Chan@cityu.edu.hk)

Abstract. Heterogeneous uptake is one of the major mechanisms governing the amounts of short-chain alkyl-amines and ammonia (NH_3) gases resident in atmospheric particles. Molar ratios of aminium to ammonium ions detected in ambient aerosols often exceed typical gas phase ratios. The present study investigated the simultaneous uptake of dimethylamine (DMA) and NH_3 into sulfuric and oxalic acid particles at gaseous DMA/NH_3 molar ratios of 0.1 and 0.5 at 10%, 50%, and 70% relative humidity (RH). Single gas uptake and co-uptake were conducted under identical conditions and compared.

Results showed that the particulate dimethyl-aminium/ammonium molar ratios (DMAH/NH_4) changed substantially during the uptake process, which was predominantly influenced by the extent of neutralization and the particle phase state. DMA uptake and NH_3 uptake into concentrated H_2SO_4 droplets were initially similarly efficient, yielding DMAH/NH_4 that were similar to DMA/NH_3 ratios. As the co-uptake continued the DMAH/NH_4 gradually dropped due to a preferential uptake of NH_3 into still acidic droplets. Once the droplets were neutralized, the stronger base DMA displaced some of the ammonium absorbed earlier, leading to DMAH/NH_4 that were up to four times higher than the corresponding gas phase ratios. At 10% RH, crystallization of partially neutralized sulfate particles prevented further DMA uptake, while NH_3 uptake continued, and displaced $DMAH^+$ after the solid particles were completely neutralized, forming almost pure ammonium sulfate. Displacement of $DMAH^+$ by NH_3 has also been observed in neutralized, solid oxalate particles. The results illustrate why in ambient liquid aerosols the DMAH/NH_4 can be larger than DMA/NH_3, despite of an excess of NH_3 in the gas phase; the uptake of DMA to aerosols consisting of crystalline ammonium salts, however is unlikely, even if the gas concentrations of DMA and NH_3 are of the same magnitude.

1. Introduction

NH_3 and short-chain alkyl-amines (R_3N) gases are frequently detected in the atmosphere. Total emissions of NH_3 largely dominate those of R_3N (Schade and Crutzen, 1995). The characteristic ambient mixing ratios of NH_3 and R_3N are in the order of several parts per billion by volume and parts per trillion, respectively (Ge et al., 2011; You et al., 2014; Zheng et al., 2015). Many of the emission sources of R_3N such as agricultural and industrial activities also release NH_3 (Behera et al., 2013). Hence, elevated R_3N gas concentrations are likely accompanied by enhanced concentrations of NH_3 (Schade and Crutzen, 1995; Zheng et al., 2015). Despite the 2-3 orders of magnitude difference in gas phase concentration, particle phase aminium-to-ammonium (R_3NH/NH_4) molar ratios of up to 0.2 have been detected. For instance, average R_3NH/NH_4 molar ratios of 0.0045–0.17 were measured in $PM_{1.8}$ in urban and rural continental air masses over urban and rural sites in Ontario, Canada (VandenBoer et al., 2011), 0.02 in $PM_{1.0}$ in an urban area of Arizona, USA (Youn et al., 2015) and 0.23 in particles with a vacuum aerodynamic diameter of 50-800 nm in California, USA (Sorooshian et al., 2008).

Large R_3NH/NH_4 ratios in particles below 20 nm have been correlated to enhanced particle formation (VandenBoer et al., 2011; Youn et al., 2015). Laboratory studies (Almeida et al., 2013; Jen et al., 2014), field measurements (Mäkelä et al.,

Atmos. Chem. Phys. Discuss., doi:10.5194/acp-2016-995, 2016
Manuscript under review for journal Atmos. Chem. Phys.
Published: 17 November 2016

Atmospheric Chemistry and Physics Discussions

2001; Kulmala et al., 2013), as well as computational methods (Kurtén et al., 2008; Olenius et al., 2013) have indicated that clusters of sulfuric acid (H_2SO_4) and DMA are more stable than clusters formed from NH_3-H_2SO_4 nucleation, and thus R_3N may contribute more to new particle formation than NH_3. Furthermore, R_3N are able to form sulfuric acid-amine clusters by replacing NH_3 in ammonium-sulfuric acid clusters (Bzdek et al., 2010a; Bzdek et al., 2010b) and ammonium nitrate nanoparticles (Lloyd et al., 2009), despite the presence of NH_3 in the gas phase (Lloyd et al., 2009). If not directly participating in the nucleation of particles, R_3N can also efficiently partition into clusters and small particles (Kürten et al., 2016) to promote particle growth.

However, R_3N are not only detected in the nucleation mode (Mäkelä et al., 2001; Smith et al., 2008), but also in aerosols exceeding 100 nm in diameter. In fact, mass loadings of alkylaminium ions (R_3NH^+) are the highest in marine particles as well as urban and rural aerosols with a diameter of 140-560 nm (Müller et al., 2009; VandenBoer et al., 2011; Youn et al., 2015). These aminium ions were observed to be internally mixed with sulfate, nitrate or organic acids (Sorooshian et al., 2008; Müller et al., 2009; Pratt et al., 2009; Smith et al., 2010; VandenBoer et al., 2011; Healy et al., 2015; Youn et al., 2015), suggesting that heterogeneous reactions forming aminium salts are an important sink for atmospheric R_3N (You et al., 2014; Tao et al., 2016). On the other hand, enhanced NH_4^+ concentrations in particles of the accumulation mode typically dominate R_3NH^+ concentrations, leading to low observed R_3NH/NH_4 molar ratios. A second peak of R_3NH/NH_4 in the coarse mode has been reported (VandenBoer et al., 2011; Youn et al., 2015), although the causes of these higher ratios in larger particles are not resolved to date.

Chemical characteristics of R_3N and their salts can deviate significantly from those of NH_3 and its salts. For instance, due to the electron donor effect of the alkyl groups, the nitrogen atom of R_3N molecules is more nucleophilic towards hydronium ions, making them stronger bases than NH_3 (Breitmaier and Jung, 2005). Furthermore, short-chain methyl- and ethyl-aminium nitrates, chlorides, and sulfates possess higher osmotic coefficients than their ammonium counterparts (Bonner, 1981; Macaskill and Bates, 1986; Chu et al., 2015; Sauerwein et al., 2015; Rovelli et al., 2016), which increases the aerosol hygroscopicity and liquid water content. Besides, secondary and tertiary aminium sulfates remain in the liquid state even at RH below 3% (Chan and Chan, 2013) and they effectively lower the deliquescence RH of the particles when mixed with ammonium sulfate (Qiu and Zhang, 2012). Particles with a large R_3NH/NH_4 ratio are consequently less acidic and could absorb more water than ammonium sulfate ($(NH_4)_2SO_4$), even at low RH.

Particulate R_3NH^+ concentrations in ambient aerosols are positively correlated with particle acidity, liquid water content, and RH (Sorooshian et al., 2008; Rehbein et al., 2011; VandenBoer et al., 2011; Youn et al., 2015). Numerous laboratory uptake experiments of R_3N into H_2SO_4 (Wang et al., 2010), ammonium nitrate, sulfate and bisulfate have confirmed such correlations (Lloyd et al., 2009; Bzdek et al., 2010b; Qiu et al., 2011; Chan and Chan, 2012, 2013). However, the conditions in those experiments would also promote heterogeneous uptake of NH_3 (Swartz et al., 1999). Although there are many studies on the uptake of either NH_3 (Huntzicker et al., 1980; McMurry et al., 1983; Daumer et al., 1992; Swartz et al., 1999; Hanson and Kosciuch, 2003; Liggio et al., 2011) or R_3N (Bzdek et al., 2010a; Bzdek et al., 2010b; Wang et al., 2010; Bzdek et al., 2011; Qiu et al., 2011; Chan and Chan, 2012) into acidic particles, to date none has been reported on the simultaneous uptake of NH_3 and R_3N.

Barsanti et al. (2009) were the first to model the relative importance of R_3N (using DMA as a model compound) and NH_3 in gas-particle partitioning. They showed that even when NH_3 gas phase concentrations exceeded those of R_3N by an order of magnitude, aminium R_3NH^+ can still dominate NH_4^+ in the aqueous acetic acid particle, due to their stronger basicity. Yet,

Atmos. Chem. Phys. Discuss., doi:10.5194/acp-2016-995, 2016
Manuscript under review for journal Atmos. Chem. Phys.
Published: 17 November 2016

Atmospheric Chemistry and Physics Discussions

owing to the lack of chemical and physical parameters available, the study relied strongly on estimations of group contributions.

The present study is the first to investigate the simultaneous uptake of R_3N and NH_3 by acidic particles with analysis of particle phase composition. We explored the temporal changes in R_3NH/NH_4 molar ratios during the uptake of DMA and NH_3 into H_2SO_4 and oxalic acid ($H_2C_2O_4$) particles at different DMA/NH_3 gas ratios (0.1 and 0.5) and RH (10% and 50% RH). We used supermicron particles because they enabled a longer observation window and sufficient mass concentrations for studying the temporal changes in particle composition during the uptake until equilibrium was reached. The results also reveal the influence of the extent of neutralization and the change in phase state on the uptake behavior of both gases. DMA was chosen as the model R_3N due to its atmospheric abundance (Müller et al., 2009; Rehbein et al., 2011; Hu et al., 2015; Youn et al., 2015) and unique characteristics, such as forming a non-crystallizing DMAS droplet even at low RH (Chan and Chan, 2013) and its higher hygroscopicity than that of $(NH_4)_2SO_4$.

2. Methods

Supermicron particles deposited on a hydrophobic substrate were placed in a temperature- and humidity-controlled flow-cell coupled to a Raman microscope setup (Yeung et al., 2009). DMA and NH_3 at low ppm levels were generated by directing a humidified N_2 carrier flow through permeation tubes holders containing tubes filled with pure liquefied NH_3 and DMA at controlled temperatures. The two gases were mixed and introduced to four cells in parallel. Post reaction samples were analyzed by ion chromatography (IC). R_3N and NH_3 gas molecules and aminium ions in solution tend to adsorb on surfaces (Dawson et al., 2014; Hansen et al., 2013; Robacker and Bartelt, 1996). To ensure accuracy of the gas ratio, measures were taken including conditioning the setup for a prolonged period, separating RH conditioning cells and reaction cells. A schematic of the experimental setup is shown in the supplemental information Fig. S1.

2.1 Generation and detection of NH_3 and DMA gases

A humidified N_2 carrier flow was directed into two electronic mass flow controllers (MKS Instruments Inc., GE50A) at 1000 ± 10 cm^3 min^{-1} and subsequently introduced into glass permeation tube holders (Fig. S1). The tube holders consisted of a water coated coil and a chamber containing the permeation tubes of either NH_3 or DMA (VICI Metronics, Dynacal), as well as a thermocouple to regulate the temperature to 293.3±0.2 K. Permeation rates were determined gravimetrically to calculate the mixing ratio of each gas.

Combination of the DMA flow (0.15 or 0.9-1.0 ppm) and the NH_3 flow (1.8-1.9 ppm) resulted in DMA/NH_3 ratios of 0.07±0.01 and 0.46±0.04 at 10% RH, as well as 0.07±0.01 and 0.49±0.02 at 50% RH (Table 2), and 0.49±0.02 at 10% and 0.52±0.01 at 70% RH for experiments with $H_2C_2O_4$. We denote these experimental conditions for uptake into H_2SO_4 by $0.1_{10\%}$, $0.5_{10\%}$, $0.1_{50\%}$, and $0.5_{50\%}$, and for uptake into $H_2C_2O_4$ by $ox0.5_{10\%}$ and $ox0.5_{70\%}$. For co-uptake gas flows from both permeation devices were mixed and split equally into four custom-made PTFE flow cells. Single gas flows were generated by bypassing one of the permeation tubes. The cells were maintained at 296.3±1.0 K and RH of 10%±2% and 50%±3%. The system including the PTFE cells was equilibrated with the NH_3 and/or DMA gas for > 12 h before the start of each experiment. The stability of the generated gas concentrations arriving at the PTFE cells was confirmed by ion-molecule reaction mass spectrometry (IMR-MS, AirSense, V&F Analyse-und Messtechnik GmbH).

Atmos. Chem. Phys. Discuss., doi:10.5194/acp-2016-995, 2016
Manuscript under review for journal Atmos. Chem. Phys.
Published: 17 November 2016

Atmospheric Chemistry and Physics Discussions

2.2 Particle generation

The stock solutions of 30 wt% H_2SO_4 or saturated $H_2C_2O_4$ were prepared from ultrapure water (18.2 MΩ) and concentrated H_2SO_4 (97 wt%, Acros Organics, titrated against standardized NaOH) or $H_2C_2O_4$ powder (99%, Aldrich). For each experiment, a few mL of the solution were drawn into a piezoelectric particle generator (MicroFab Tech., Inc.). Approximately 2000±100 droplets of 60 µm in diameter were deposited on a hydrophobic film (FEP membranes, YSI Inc.) The sample was then inserted into a clean flow cell connected to humidified high purity N_2 (~1000 cm^3min^{-1}) to equilibrate to either 10 or 50% RH for 45 min. The sample films were subsequently transferred into the PTFE reaction cells. RH conditioning and transfer of films took place inside a glove bag (GLOVEBAG, Glas Col®) to avoid exposure of the samples to room air and humidity.

2.3 Particle analysis

For each condition, the experiment was repeated in different time intervals to complete one time series. The samples were removed from the cell and submerged in ~12 mL of ultrapure water for extraction and subsequent chemical analysis. Both cation and anion contents were measured by IC (Metrohm, 881 compact IC Pro) as described by Sauerwein et al. (2015).

IC yields total values for DMA and NH_3 species, and hence the distribution between molecules and ions in the samples could not be determined. In the following we use DMAH to represent $n NH_2(CH_3)_2^+ + n NH(CH_3)_{2(aq)}$ and NH_4 to represent $n NH_4^+ + n NH_{3(aq)}$ in the particles, where n denotes the molar amounts of each compound. The same is true for the distribution between acidic species. Hereafter the molar amount of the total sulfate is indicated by $SO_4 = n H_2SO_4 + n HSO_4^- + n SO_4^{2-}$, and the total oxalate as C_2O_4. Molar ratios in the particle phase are accordingly denoted by DMAH/NH_4, DMAH/SO_4, and NH_4/SO_4, while gaseous molar ratios are denoted by DMA/NH_3.

DMAH concentrations of the first measurement points for particles in the $0.1_{10\%}$ and $0.1_{50\%}$ conditions lay at the lower end of the IC calibration range. A conservative estimation of up to 15% uncertainty for these values would decrease the DMAH/NH_4 ratio by 0.02, which has negligible impacts on the observed trends and values (see Fig.3).

After 35-38 hours, samples showed no significant changes in particle composition and were thus considered to be in equilibrium. Equilibrated samples were divided into two groups, with one directly undergoing IC analysis and the other placed in clean cells under an N_2 atmosphere for > 5 hours prior to IC analysis to further investigate their compositional stability.

Furthermore, uptake experiments at $0.5_{10\%}$ and of NH_3 at 10% RH were repeated with particles of 60-200 µm in size in flow cells equipped with a quartz window to track alterations in chemical composition and concurrent morphological changes with a Raman microscope (Renishaw RM series) as described by Yeung et al. (2009) and Chu et al. (2015). A 20 mW Argon ion laser (514.5 nm) was deployed for sample excitation and a 1800 g mm^{-1} grating was selected to obtain spectra in the range of 200 to 4000 cm^{-1} with a resolution of 1.4 cm^{-1}.

3. Results and discussion

Uptake of NH_3, DMA and their mixtures into H_2SO_4 particles were conducted at 10% and 50% RH. Single component uptake served as the base case for comparison. Additional experiments with $H_2C_2O_4$ at 10 and 70% RH were conducted at a gas ratio of 0.5 only and are discussed in Sect. 3. A summary of all the experimental conditions is given in Table 1.

Atmos. Chem. Phys. Discuss., doi:10.5194/acp-2016-995, 2016
Manuscript under review for journal Atmos. Chem. Phys.
Published: 17 November 2016

Atmospheric Chemistry and Physics Discussions

The uptake of alkaline gases into acidic droplets involves a series of inter-related processes including gas phase diffusion, immediate reaction of gas molecules colliding with the aerosol surface (Eq. 1a and b) or adsorption and dissolution (Eq. 2a and b), followed by further liquid phase diffusion and proton transfer in the bulk particle (Eq. 3a and b) (Swartz et al., 1999; Kulmala and Wagner, 2001; Davidovits et al., 2006; Pöschl et al., 2007; Kolb et al., 2010).

$$NH_{3(g)} + H_3O^+_{(surface)} \rightleftharpoons NH_4^+{}_{(sf)} + H_2O \quad (1a)$$

$$NH(CH_3)_{2(g)} + H_3O^+_{(surface)} \rightleftharpoons NH(CH_3)_2H^+{}_{(sf)} + H_2O \quad (1b)$$

$$NH_{3(g)} + H_2O \rightleftharpoons NH_{3(aq)} + H_2O \quad (2a)$$

$$NH(CH_3)_{2(g)} + H_2O \rightleftharpoons NH(CH_3)_{2(aq)} + H_2O \quad (2b)$$

$$NH_{3(aq)} + H_3O^+ \rightleftharpoons NH_4^+{}_{(aq)} + H_2O \quad (3a)$$

$$NH(CH_3)_{2(aq)} + H_3O^+ \rightleftharpoons NH(CH_3)_2H^+{}_{(aq)} + H_2O \quad (3b)$$

The above equations and related reaction steps indicate a strong acidity dependence, thus with increasing neutralization, the scope of DMA and NH_3 uptake may change. Here, the extent of (stoichiometric) neutralization of the particles is defined as the number of moles of alkaline species over moles of acidic species, $X = (DMAH+NH_4)/SO_4$ or $X = (DMAH+NH_4)/C_2O_4$ and is hereafter referred to as the neutralization ratio. In the course of the uptake experiments, the neutralization ratio ranged from highly acidic ($X = 0$) to neutral ($X = 2$). But not all equilibrated particles were completely neutralized, as will be further discussed in Sect. 4.

3.1 Single gas uptake

At 50% RH, the uptake of NH_3 fully neutralized the H_2SO_4 droplets within 2 hours, forming aqueous $(NH_4)_2SO_4$ droplets (Fig. 1, grey diamonds). At 10% RH, NH_3 uptake (Fig. 1, open diamonds) was similar to that at 50% RH initially, until X exceeded 1.1, where crystallization significantly retarded the subsequent uptake. The continued increase in particulate NH_4^+ even after crystallization indicates that crystalline acidic particles were still susceptible to uptake, but imposed bulk diffusion limitations that retarded the uptake. Neutralization was not complete within the measured period of 15 hours.

Uptake of DMA at the mixing ratio of 0.15 ppm (Fig. 1, triangles) was significantly slower than that at 1 ppm (Fig. 1, squares). Like the initial uptake of NH_3, DMA uptake did not differ significantly between 10% and 50% RH, until approaching equilibrium at DMAH/SO_4 ratios of 1.5±0.1 at 10% RH, and 1.7±0.1 ($DMA_{0.15ppm}$) and 1.9±0.1 (DMA_{1ppm}) at 50% RH (Table 1, X_{equil}). There was no indication of phase change in these particles even at 10% RH. This is consistent with earlier studies, where secondary and tertiary methyl and ethyl-aminium sulfates were described as hygroscopic, non-crystallizing salts at RH ≤ 10% (Qiu and Zhang, 2012; Chan and Chan, 2013; Chu et al., 2015). Furthermore, these studies showed that upon drying of synthesized DMAS droplets (DMAH/SO_4 ratios = 2) with amine-free air, DMA evaporated from the particles, leading to a final DMAH/SO_4 ratio of 1.5 at < 3% RH (Chan and Chan, 2013; Chu et al., 2015). In our experiment, the same equilibrium DMAH/SO_4 ratio of 1.5 was established at 10% RH, despite a continuous supply of DMA gas.

Particles exposed to 1 ppm of DMA at 10% RH were more neutralized initially with $X_{max\ neutral} = 1.7±0.1$ (Table 1,) and then equilibrated to lower X_{equil} of 1.5±0.1 (Table 1). Some of the initially absorbed DMA molecules had re-partitioned into the gas phase despite the presence of DMA gas in the surrounding atmosphere. The phenomenon of re-volatilization is further discussed in Sect. 4.

Atmos. Chem. Phys. Discuss., doi:10.5194/acp-2016-995, 2016
Manuscript under review for journal Atmos. Chem. Phys.
Published: 17 November 2016

Atmospheric Chemistry and Physics Discussions

3.2 DMA-NH_3 co-uptake

Figure 2 depicts the temporal profiles of DMAH/SO_4, NH_4/SO_4 and *X* at the different gas ratios and RH. At 10% RH particles solidified during the experiment (Fig. 2a and b, indicated by crosshatched areas) and needed 2 to > 18 hours (for $0.5_{10\%}$ and $0.1_{10\%}$, respectively) to completely neutralize SO_4. Upon reaching neutralization, NH_3 had almost completely displaced the DMAH absorbed earlier from the solid particles. The phase transition and DMAH displacement at 10% RH will be further discussed in Sect. 2.3 and 2.4.

At 50% RH SO_4^{2-} was completely neutralized (Fig. 2c and d) within 1-2 hours. Neutralization in droplets was followed by a partial displacement of NH_4 by DMA, reaching a final equilibrium composition enriched in DMAH (Sect. 2.2). The results show that the DMAH/NH_4 ratios varied substantially during uptake before stable compositions were reached. In the following, we will discuss the dependence of gas uptake on the phase state and neutralization ratio of the particles.

3.2.1 Uptake into liquid acidic droplets

Figure 3 displays the changes in the DMAH/NH_4 ratios as a function of time for the four co-uptake experiments. For the first measurement point under each condition, the DMAH/NH_4 ratio (Table 2, $t_{initial}$) was close to the gas phase DMA/NH_3 ratio (indicated by grey bands in Fig. 3), implying that initially both gases partitioned equally effectively into highly concentrated H_2SO_4. For instance, in panels a and b the DMAH/NH_4 ratios in the acidic droplets were 0.07±0.01 and 0.43±0.04, comparable to gaseous DMA/NH_3 ratios of 0.07 and 0.46, respectively.

Swartz et al. (1999) measured the heterogeneous uptake of NH_3 into a chain of 70 wt% and 40 wt% H_2SO_4 droplets (equilibrated at 10% and 50% RH, respectively), and obtained gas phase diffusion-corrected uptake coefficients (γ_{NH3}) of 0.8 and 1.0, respectively. The highly effective uptake into concentrated H_2SO_4 at pH < 0 was attributed to surface reactions, i.e., NH_3 molecules reacting with interfacial hydronium ions (H_3O^+) without prior solvation (Swartz et al., 1999). As H_2SO_4 droplets in the present study have a solution pH ≤ - 0.9 (Wexler and Clegg, 2002) at both 50% RH (43 wt% H_2SO_4) and 10% RH (64 wt% H_2SO_4), protonation without prior dissolution may take place for NH_3 in the first few minutes of uptake when pH is very low.

To date no systematic study on the relevance of surface protonation has been conducted for DMA uptake. However the gas phase basicity of NH_3 and its derivatives (such as R_3N) have been shown to correlate well with the differential heats of chemisorption on acidic (zeolite) surfaces (Parrillo et al., 1993). Since DMA possesses a slightly higher gas phase basicity than NH_3 (Brauman et al., 1971; Parrillo et al., 1993), DMA gas molecules might, similar to NH_3, have a high affinity to interfacial H_3O^+. Surface protonation on fresh H_2SO_4 particles may thus be important for the initial uptake of both NH_3 and DMA, which could explain why the initial particle phase ratio is equal to the gas phase ratio.

Wang et al. (2010) reported an uptake coefficient (γ_{DMA}) of about 0.03 for DMA uptake into concentrated H_2SO_4 of ≥ 62 wt% (≤ 10% *RH*) at 283 K, which is noticeably smaller than the coefficient of close to unity reported for NH_3 uptake into H_2SO_4 of similar acidity (Swartz et al., 1999). In the current study, NH_3 uptake into fresh H_2SO_4 droplets was not overwhelmingly dominant. However, as the uptake continued, the DMA/NH_4 ratios dropped by 30-40% for all experimental conditions within the first 1-2 hours (Fig. 3 a-d), which indicates a preferential uptake of NH_3. Since the gas concentrations of both NH_3 and DMA were constant, it is likely that the decreasing particle acidity and increasing neutralization ratio caused this change. Swartz et al. (1999) reported a threshold pH ≤ 0 for surface protonation to occur and a drop in γ_{NH3} by one order of magnitude when the pH was increased to above zero. Hanson and Kosciuch (2003) observed a similar drop in γ_{NH3} during the uptake of NH_3 into H_2SO_4, when the solution approached ammonium bisulfate (NH_4HSO_4) composition.

Atmos. Chem. Phys. Discuss., doi:10.5194/acp-2016-995, 2016
Manuscript under review for journal Atmos. Chem. Phys.
Published: 17 November 2016

Atmospheric Chemistry and Physics Discussions

Using the *E-AIM* model (Wexler and Clegg, 2002, *www.aim.env.uea.ac.uk/aim*) we estimated that nH_3O^+ decreased by about 40% as the neutralization ratio increased from $X = 0$ (H_2SO_4 droplets) to 0.5. Once the particles were half neutralized ($X = 1$, bisulfate stoichiometry), the solution pH were estimated to exceed zero. Hence if we assume a similar threshold as reported by Swartz et al. (1999), surface protonation (Eq. 1a and b), which can explain the comparable initial uptake of DMA and NH_3, may no longer be relevant when particles approached bisulfate composition.

Figure 4 compares the uptake of DMA and NH_3 in single and mixed gas experiments. The uptake trends of single gas and co-uptake did not deviate noticeably, confirming that DMA and NH_3 uptake took place independent of each other. Despite the increase in pH when neutralization ratios exceeded unity ($X = 1$), there were sufficient amounts of H_3O^+ to support the uptake of both gases. Hence, the presence of NH_3 gas molecules at 14 times higher concentration than DMA had little effect on the uptake of DMA into acidic particles. The same can be said for DMA, which seemed not to have influenced NH_3 partitioning into acidic droplets. This finding clearly differentiates the group of hydrophilic R_3N from more hydrophobic organics such as hexadecane, hexadecanol (Daumer et al., 1992) or typical atmospheric organic vapor (Liggio et al., 2011), which form an organic film that limits the access of NH_3 to the inorganic core.

The independent uptake of DMA and NH_3 at 10% RH prevailed until the particles underwent phase change (Fig. 4a and c, dotted lines). Once particles effloresced, a preferential uptake of NH_3 was observed, which resulted in a significant drop in DMAH/NH_4 (Fig. 3a and b), as discussed in Sect. 2.3. At 50% RH the co-uptake of DMA and NH_3 was independent from each other until the particles reached complete neutralization ($X = 2.0$) (Fig. 4b and d, solid lines). Once neutralized, only DMA uptake continued (Fig. 4b) with concurrent displacement of NH_4^+ (Fig. 4d) as discussed hereafter.

3.2.2 Displacement of NH_4^+ from neutralized droplets

When approaching full neutralization, where both gases started to compete for limited available H_3O^+ ions, the DMAH/NH_4 ratios in droplets of the $0.1_{50\%}$ and $0.5_{50\%}$ experiments started to increase (Fig. 3c and d, solid line). In solution DMA (pK_a= 10.64; Hall, 1957) is a stronger base than NH_3 (pK_a = 9.21), consequently it has a higher affinity for H_3O^+ than NH_3 does. Thus, while the fraction of DMA species gradually increased, some of the NH_4^+ dissociated (Eq. 3a, reverse reaction) and NH_3 was released back to the gas phase (Eq. 2a, reverse reaction).

Similar displacement of NH_4^+ by alkyl-amines has been reported for aqueous particles of ammonium bisulfate, chloride, oxalate and sulfate at 50 and 75% RH (Chan and Chan, 2012, 2013) and nitrate at 20% RH (Lloyd et al., 2009). Similarly, Lloyd et al. (2009) observed the displacement of NH_4^+ by trimethylamine (TMA) from water-coated NH_4NO_3 nanoparticles despite an excess of NH_3 gas ($n\text{TMA}_{(g)}/n\text{NH}_{3(g)} = 0.1$), although they did not report the quantity of NH_4^+ displaced. Their gas phase conditions were comparable to our experiment at $0.1_{50\%}$. In our experiment DMA was able to displace about 9% of the initially absorbed NH_4^+ (Table 2, χ_{NH4+}). The equilibrium DMAH/NH_4 ratio in the $0.1_{50\%}$ condition was 0.18±0.02 (Table 2, t_{equil}), which indicates an enhancement of DMA by a factor of 2-3 in the particle phase compared to the gas phase. Particles under $0.5_{50\%}$ conditions equilibrated at a DMAH/NH_4 ratio of 1.77±0.13, hence 3-4 times higher than the gas ratio; by the time a stable particle composition was established, 50% of the initially absorbed NH_4^+ was displaced (Table 2). Yet it should be noted that equilibrated particles at $0.5_{50\%}$ possessed a neutralization ratio of only $X = 1.8$±0.1, hence the particle was incompletely neutralized (see Sect. 4) despite the presence of 1.9 ppm NH_3 and 0.9 ppm DMA in the surrounding gas phase.

The experimental equilibrium DMA/NH_3 and DMAH/NH_4 ratios (Table 2, t_{equil}) were compared with calculations using the *E-AIM* Model (Model II, 296 ± 1 K, no solid formation; Wexler and Clegg, 2002). Measured equilibrium DMAH/SO_4, NH_4/SO_4 were used as input parameters. The *E-AIM* predicted DMA/NH_3 gas ratios that would equilibrate over particles lay

Atmos. Chem. Phys. Discuss., doi:10.5194/acp-2016-995, 2016
Manuscript under review for journal Atmos. Chem. Phys.
Published: 17 November 2016

Atmospheric Chemistry and Physics Discussions

with DMA/NH_3 of 0.14 and 0.01, below the experimental DMA/NH_3 gas ratios of 0.49 and 0.07. Considering the entire uptake process, the modelled result would imply a more intensive displacement of NH_4^+ by DMA and stronger enrichment of DMA relative to NH_3 species in the particle phase compared to the gas phase. Yet, the experimental findings are qualitatively consistent with the *E-AIM* - modeled values and with earlier simulations by Barsanti et al., (2009), who reported that $DMAH/NH_4$ in submicron acetic acid droplets can be significantly larger than their gas phase ratio, even if gas concentrations of NH_3 dominated DMA by one to three order of magnitudes.

Thus, in the current study we provide experimental evidence that DMA preferentially partitions into neutralized liquid sulfate particles over NH_3, due to its stronger alkalinity. DMA then partially displaces NH_4^+ from neutralized aqueous particles even when the NH_3 gas concentration is one order of magnitude greater than the DMA gas concentration.

3.2.3 Phase transition and uptake into solid acidic particles

NH_3 (single gas) uptake into H_2SO_4 at 10% RH decelerated noticeably when the NH_4/SO_4 ratio exceeded 1.1 (Fig. 5, filled triangles). A comparable retardation occurred in the co-uptake experiments $0.1_{10\%}$ and $0.5_{10\%}$, but at NH_4/SO_4 ratios of about 1.5 (Fig. 5a and b, open triangles).

We used Raman microscopy (Chu et al., 2015) to further investigate the slowdown of the reactions and possible changes in the physical state for the single uptake of NH_3 (Fig. 6) and the co-uptake experiment $0.5_{10\%}$ (Fig. 7). Note that each sample was composed of several hundreds of closely packed droplets deposited on a substrate. The droplets were not expected to reach the same cation-to-sulfate stoichiometry, nor exhibit phase transitions at the exact same time. For the acquisition of in-situ Raman signals, we selected individual particles just before and right after phase transition, and in crystalline state, to represent the phase change process.

During the single gas uptake of NH_3 into H_2SO_4 droplets at 10% RH, crystallization occurred within the first 60 min. As shown in Fig. 6, during efflorescence of acidic droplets (Fig. 6, spectra 2 and 3) the HSO_4^- characteristic bands at 590 cm^{-1} and 1035 cm^{-1} (Dawson et al., 1986; Lund Myhre et al., 2003) transformed to doublets at 579/609 cm^{-1} and 1013/1043 cm^{-1} of solid particles (Fig. 6, spectra 2 and 3), suggesting the formation of crystalline NH_4HSO_4 (Dawson et al., 1986; Colberg et al., 2004). As uptake continued, a gradual shift towards $(NH_4)_2SO_4$ was indicated by an increase in the SO_4^{2-} stretching mode 975 cm^{-1} and a decrease in the HSO_4^- band at 579 cm^{-1} (Fig. 6, spectrum 4). The retarded diffusion of NH_3 from the surface to the interior of the crystals is likely to have limited the uptake, explaining why the spectra did not fully resemble $(NH_4)_2SO_4$ (Fig. 6, spectrum 5) within the measured period.

Efflorescence was also observed for the co-uptake of NH_3 and DMA at 10% RH. Under $0.5_{10\%}$ conditions, most particles experienced the first morphological change after 40–60 min of uptake, forming fairly spherical solids with long lined patterns (Fig. 7, yellow rectangular). Raman spectral analysis of particles that had only just transitioned from liquid to solid phase state (Fig. 7, spectrum 3) showed an emerging SO_4^{2-} band at 984 cm^{-1}. Meanwhile the HSO_4^- frequencies near 590 cm^{-1} and 1030 cm^{-1} in the droplet (Fig. 7, spectrum 2) shifted towards 597 cm^{-1} and 1043 cm^{-1} in the solid particle (Fig. 7, spectrum 3) but both remained single broad peaks, without signs of scissoring as observed for bisulfate from NH_3 single gas uptake (Fig. 6, spectra 3 and 4). The observed features more closely resemble the spectral characteristics of letovicite $(NH_4)_3H(SO_4)_2$ (Colberg et al., 2004) than those of NH_4HSO_4 or $(NH_4)_2SO_4$.

The during NH_3-DMA co-uptake the absorbed $DMAH^+$ seems to have suppressed NH_4HSO_4 precipitation in particles with a composition of $1.1 < NH_4/SO_4 < 1.5$, so that the phase change started only at a NH_4/SO_4 around 1.5 (Fig. 5a and b). It can be seen from the $0.1_{10\%}$ experiment (Fig. 5a) that this suppression of NH_4HSO_4 precipitation also occurred if the $DMAH/NH_4$ at

Atmos. Chem. Phys. Discuss., doi:10.5194/acp-2016-995, 2016
Manuscript under review for journal Atmos. Chem. Phys.
Published: 17 November 2016

Atmospheric Chemistry and Physics Discussions

the time of phase change was as low as 0.05 (Table 2, t_{pc}), hence even if the concentration of DMA species was low compared to the amount of NH_3 species present in the particle. Since R_3NH/NH_4 ratios in ambient samples near emission sites can be up to 0.23 (Sorooshian et al. 2008), and with $DMAH^+$ as the most frequently detected aminium ion in aerosols (Müller et al., 2009; Rehbein et al., 2011; Hu et al., 2015; Youn et al., 2015) $DMAH/NH_4$ ratios in aerosols can possibly reach ≥ 0.05 and thus could change the crystallization behavior of NH_4–H–SO_4–salts in atmospheric particles.

By retaining the particles of a composition of $1.1 < NH_4/SO_4 < 1.5$ at 10% RH in liquid phase, the presence of DMA species accelerated the uptake of NH_3 compared to single gas NH_3 uptake where crystallization retarded the uptake into particles with $NH_4/SO_4 > 1.1$.

After the NH_4–DMAH–mixed particles crystallized, the uptake of NH_3 continued at a slower pace (Figure 5a and b), while DMA was no longer absorbed and the $DMAH/NH_4$ ratio started to decrease (Fig. 3a). In earlier reports of single gas R_3N uptake (where R_3N might be methylamine, DMA, TMA or triethylamine) R_3N (in the absence of NH_3) were observed to effectively adsorb onto NH_4HSO_4 surfaces in a coated flow reactor (Qiu et al., 2011). In the presence of NH_3 in our experiments, however, DMA was not taken up by acidic crystalline particles. Liu et al. (2012) reported steric effects to influence the uptake effectiveness of primary, secondary and tertiary methyl-amines into solid citric and humic acid measured in a Knudsen cell reactor, where smaller R_3N molecules are more effectively absorbed than larger ones. A similar effect of steric hindrance may have caused the preferential uptake of the smaller NH_3 molecules over DMA in our experiments. Besides steric reasons, the release of lattice enthalpy during the formation of $(NH_4)_3H(SO_4)_2$ and $(NH_4)_2SO_4$ may have made the uptake of NH_3 also thermodynamically favorable.

$DMAH/NH_4$ ratios at the time of neutralization ($t_{neutral}$) reached 0.03±0.00 for the $0.1_{10\%}$ condition and 0.19±0.01 for the $0.5_{10\%}$ condition (Table 2), showing a slight enrichment of NH_4^+ in the particle over the gas phase.

3.2.4 Displacement of $DMAH^+$ from solid neutralized particles

After reaching full neutralization, both Raman spectral analysis and IC results of solid particles indicated a gradual reduction of DMA species and increase of NH_3 species in the particle phase, which is also reflected in decreasing $DMAH/NH_4$ ratios in Fig. 3a and b.

10–20 minutes after the phase transition, $DMAH^+$–NH_4^+–mixed particles experienced a second morphological change to a polycrystalline structure (Fig. 7, grey rectangular). Raman spectra of these particles showed a slowly vanishing HSO_4^- band at 1043 cm^{-1}. However, a significant decrease in the full width at half maximum (FWHM) of the SO_4^{2-} band at 980 cm^{-1}, which indicates the (full) crystallization of sulfate (Lee et al., 2008), was only observed hours after the morphology change (Fig. 7, spectrum 4). We suspect that the observed morphological changes are related to the formation of a $(NH_4)_2SO_4$ shell structure due to $DMAH^+$ displacement by NH_3. $DMAH^+$ was subsequently slowly displaced from the particle core, which eventually led to the formation of crystalline $(NH_4)_2SO_4$ with only traces of $DMAH^+$ left inside the particles.
It is interesting to note, that the $DMAH/NH_4$ ratios of equilibrated particles for $0.5_{10\%}$ and $0.1_{10\%}$ were both 0.02 (Table 2). Even if the NH_3 gas concentration is only twice of that of DMA, NH_3 can almost completely displace $DMAH^+$ from the solid particle.

Since different gas mixtures resulted in similar particle composition, calculations by *E-AIM* based on these equilibrated particle compositions yielded similar gas phase DMA/NH_3 ratios for the $0.1_{10\%}$ and $0.5_{10\%}$ experiments of 0.57 and 0.32, with an uncertainty of up to 40% due to strong temperature sensitivity. The modelled results are qualitatively in agreement

Atmos. Chem. Phys. Discuss., doi:10.5194/acp-2016-995, 2016
Manuscript under review for journal Atmos. Chem. Phys.
Published: 17 November 2016

Atmospheric Chemistry and Physics Discussions

with the experimental results, confirming that despite considerable amounts of DMA in the gas phase, the equilibrated solid sulfate particle would predominantly contain NH_3 species.

Overall it can be concluded that, for DMA-NH_3 co-uptake, NH_3 is favorably absorbed into acidic liquid particles, except for very concentrated H_2SO_4, where DMA and NH_3 seem to partition similarly effectively. Unless the particles either crystallize or are close to full neutralization, DMA and NH_3 in general do not influence each other's uptake and act as if they were the only gas present.

For uptake into neutralized particles, DMA is favorably absorbed into liquid neutral particles due to its stronger basicity leading to partial NH_4^+ displacement depending on gas phase NH_3 concentration; NH_3 is favorably taken up into solid neutral particles and can almost completely displace $DMAH^+$ due to the thermodynamically favorable formation of $(NH_4)_2SO_4$ crystals and steric reasons.

3.3 Uptake into oxalic acid particles

We performed additional experiments with $H_2C_2O_4$ to further elucidate the influence of phase state on the co-uptake process. $H_2C_2O_4$ is a model organic acid frequently detected in ambient aerosols (Kawamura and Ikushima, 1993; Decesari et al., 2000; Yao et al., 2003; Yu et al., 2005; Müller et al., 2009) . Efflorescence of aqueous supermicron $H_2C_2O_4$ particles occurs at 51.8%-56.7% RH, forming anhydrous solids (Peng et al., 2001). We chose to examine the co-uptake of DMA and NH_3 into initially solid and initially liquid particles, respectively, at 10% and 70% RH.

Figure 8 compares the co-uptake into $H_2C_2O_4$ and H_2SO_4 particles at DMA/NH_3 = 0.5. Within the first hour of uptake into solid $H_2C_2O_4$ particles at 10% RH (Fig. 8a, inverted triangles), the neutralization ratio increased to X = 0.3. In the subsequent 15 hours, no further increase occurred, suggesting that the gas uptake into anhydrous $H_2C_2O_4$ particles was incomplete and may have been limited to adsorption on the surface and outer layers of the particles. DMAH/NH_4 ratios decreased from initially 0.26±0.05 during the first four hours of uptake to 0.17±0.04 after 14-15 h (Table 2), despite a relatively constant overall neutralization ratio (X = 0.3). Some of the initially ad-/absorbed DMA molecules were displaced by NH_3.

The uptake at 70% RH starting with $H_2C_2O_4$ droplets was monitored under the microscope for subsequent phase changes (Fig. S2). Within 15 minutes of uptake, liquid particles transformed into round, irregularly patterned solids, suggesting that the uptake of even small amounts of gas caused a phase change in these $H_2C_2O_4$ particles. The formation of ammonium salts via the uptake of NH_3 has earlier been shown to decrease the hygroscopicity of $H_2C_2O_4$ particles and influence their phase state (Peng and Chan, 2001; Ma et al., 2013). We found that prior to phase change, a ring of small satellites formed around the droplets. This observation can be most plausibly explained by a pinning effect caused by fast evaporation of the solvent from a droplet deposited on a substrate (Deegan et al., 1997). Similar halo formation has been described for other atmospheric particles (Hamacher-Barth et al., 2016), yet, we believe that this effect does not have a signifincant impact on the general uptake observations here. The co-uptake trends into solidified $H_2C_2O_4$ particles at the ox$0.5_{70\%}$ conditions were comparable to those of $0.5_{10\%}$ and $0.5_{50\%}$ into H_2SO_4 (Fig. 8b), indicating that the solids formed during phase change (dashed lines, Fig. 8) did not retard the uptake and that diffusion inside the particle bulk was not a limiting factor of the uptake. In fact, the particles almost completely neutralized within the first hour of reaction. Similar observations have been reported by Li et al. (2015), who investigated NH_3 uptake into submicron organic particles produced from oxidation of isoprene, a precursor gas of $H_2C_2O_4$ (Ervens et al., 2014). Li et al. (2015) showed that even at RH down to <5%, NH_3 uptake was not restricted by diffusion. Unlike the co-uptake into partially neutralized H_2SO_4 particles at 10% RH, where DMA uptake

Atmos. Chem. Phys. Discuss., doi:10.5194/acp-2016-995, 2016
Manuscript under review for journal Atmos. Chem. Phys.
Published: 17 November 2016

Atmospheric Chemistry and Physics Discussions

discontinued once the particles formed solids, uptake of DMA into solid, partially neutralized $H_2C_2O_4$ particles remained effective.

Within two hours of uptake, the solid particles of $ox0.5_{70\%}$ experienced a morphological change and transformed into crystals (Fig. S2). Concurrently, the DMAH/NH_4 ratios dropped from 0.34 to <0.1 (Table 2, t_{equil}), showing that NH_3 can displace $DMAH^+$ from neutralized oxalate particles, which may trigger the transformation to a crystalline morphology. Final particle morphologies show a centered particle with a monoclinic or orthorhombic crystal structure, a shape typical of ammonium oxalate (Blake and Clegg, 2009), and small residuals of the satellite particles (Fig. S2).

3.4 Stability of reaction products and re-volatilization of NH_3 and DMA

As shown in Sect.1, single gas DMA uptake into H_2SO_4 equilibrated with incompletely neutralized droplets at both 10% and 50% RH with X_{equil} between 1.5–1.9 (Table 1). Temporal profiles of the DMA uptake of 1ppm at 10 % RH show that DMAH/SO_4 ratios peaked after 4-5 hours (Fig. 1), reaching $X_{max\ neutral}$ of 1.7±0.1 before DMA partially re-volatilized and particles equilibrated with a more acidic composition of X_{equil} = 1.5±0.1 (Table 1). When placing equilibrated samples into amine-free atmosphere, the neutralization ratio decreased further to X_{N2} = 1.2±0.2 at 10% RH and X_{N2} = 1.7±0.2 at 50% RH, as a result of DMA evaporation from these particles (Table 1). Similar degassing of methyl and ethyl-amines from synthesized salts has been reported in earlier studies (Chan and Chan, 2013; Chu et al., 2015; Lavi et al., 2015).

To examine the influence of NH_4^+ on the volatilization of DMA from particles and the formation of partially neutralized equilibrated droplets, we compared co-uptake experiments $0.5_{10\%}$ and $0.5_{50\%}$ to single gas uptake $DMA_{1ppm10\%}$, $DMA_{1ppm50\%}$. Figure 9 illustrates the maximum neutralization, equilibrium and composition of particles exposed to RH-conditioned N_2 atmosphere for the four mentioned experiments.

Particles in co-uptake experiments reached full neutralization (Fig. 9d and j). The total cation content in particles at 10% RH at the time of neutralization was comprised of > 80% NH_4^+ (Fig. 9d). When approaching equilibrium, $DMAH^+$ was displaced by NH_3 and the NH_4^+ content increased to 98% (Fig. 9e). Although the cation composition had changed, no decrease in X beyond the margin of error was observed (Fig. 9d to e), even when particles were exposed to pure N_2 (Fig. 9f), due to the formation of a stable crystal. At 50% RH, DMA partially displaced NH_4^+ from neutralized particles, with an increase in DMAH/SO_4 from 0.7 at the point of maximum neutralization (Fig. 9j) to 1.3 at equilibrium (Fig. 9k). Accompanying the increase in $DMAH^+$ was a drop in the total neutralization ratios from X = 2 to about X = 1.8 (Fig. 9j to k), indicating that more NH_3 has degassed than was replaced by DMA. Hence while re-volatilization of DMA was responsible for the decrease in X under $DMA_{1ppm50\%}$ conditions, degassing of NH_3 could be responsible for the decrease in neutralization ratios in co-uptake experiments. Once exposed to N_2, even more NH_3 evaporated from DMAH-NH_4 mixed particles (Fig. 9k to l), which further increased the acidity of these particles.

It should be noted, that the degassing of NH_3 was negligible for particles of the $0.1_{50\%}$ condition (Fig. 2c). At the point of maximum neutralization they contained large amounts of NH_4^+ and a DMAH/NH_4 ratio below 0.1, which seem to have prevented re-volatilization.

Under exposure to N_2, X decreased in all particles that were in liquid phase state and contained large amounts of $DMAH^+$ (Fig. 9b, h, k), reflecting that the equilibrium compositions of these droplets were sensitive to changes in DMA and NH_3 gas concentrations.

Atmos. Chem. Phys. Discuss., doi:10.5194/acp-2016-995, 2016
Manuscript under review for journal Atmos. Chem. Phys.
Published: 17 November 2016

Atmospheric Chemistry and Physics Discussions

4. Summary and Conclusions

The co-uptake of DMA and NH_3 into H_2SO_4 and $H_2C_2O_4$ particles was investigated at different RH and DMA/NH_3 gas ratios. The stoichiometric neutralization ratio and physical state of the particles were the two major factors influencing DMA and NH_3 uptake.

In the uptake into fresh, very acidic H_2SO_4 droplets at 10% and 50% RH, both DMA and NH_3 partitioned effectively, leading to a DMAH/NH_4 ratio comparable to the DMA/NH_3 gas ratio. Subsequently, the DMAH/NH_4 ratio decreased as NH_3 uptake was faster. The uptake of DMA and that of NH_3 were independent of each other because of the availability of abundant acids, as long as the particles did not reach neutralization nor undergo phase change. This result may explain why the highest particulate R_3NH^+ mass concentrations are detected in acidic aerosols with low NH_4/SO_4 (Youn et al., 2015).

In fully neutralized droplets at 50% RH, the limited availability of H_3O^+ ions for acid-base reactions led to a partial displacement of NH_4^+ by the stronger base DMA. This process yielded equilibrium particle compositions enriched in $DMAH^+$ by up to four times the gas phase ratio. It also potentially explains DMA partitioning into the neutralized condensed phase despite excess NH_3 (Sorooshian et al., 2008; Lloyd et al., 2009; Rehbein et al., 2011; VandenBoer et al., 2011).

At 10% RH, the phase changed from liquid to solid during uptake. This instantly inhibited further DMA uptake, while NH_3 uptake continued. Once the particles were fully neutralized, NH_3 displaced $DMAH^+$ from crystal structures and finally formed $(NH_4)_2SO_4$ with little residual NH_4^+, regardless of the DMA gas concentrations in the surrounding. $H_2C_2O_4$ particles at 70% RH were initially liquid, but transformed into non-crystalline solids after absorbing small amounts of DMA and NH_3. Subsequent uptake was similar to that of liquid sulfate particles. The formation of solid, partially neutralized $H_2C_2O_4$ particles did not hinder DMA uptake. Fully neutralized oxalate particles then crystallized upon displacement of $DMAH^+$ by NH_3, similar to the displacement of $DMAH^+$ from crystalline sulfate particles. Anhydrous $H_2C_2O_4$ at 10% RH was rather inert and took up small amounts of DMA and NH_3, presumably by adsorption only. In solid neutralized particles, NH_3 uptake is sterically and thermodynamically favored to form $(NH_4)_2SO_4$ or ammonium oxalate crystals by displacing $DMAH^+$. Hence, once ambient aerosols are in solid state, they are unlikely to take up R_3N, even when R_3N and NH_3 gas concentrations are of the same magnitude.

In the absence of NH_4^+, DMA partially evaporated from $DMAH^+$–rich sulfate droplets. However, in the more common scenarios where NH_4^+ is present, DMA can displace NH_4^+ from neutral droplets, and cause additional NH_3 to evaporate and form non-neutralized particles. Hence, the presence of $DMAH^+$ can prevent aqueous sulfate particles from full neutralization. In our experiments NH_3 re-volatilization required DMAH/NH_4 ratio of about 0.5, which is at the upper end of DMAH/NH_4 measured in atmospheric particles (Sorooshian et al., 2008; VandenBoer et al., 2011; Youn et al., 2015).

The DMA and NH_3 gas concentrations and sulfate neutralization ratios used in the present study are high and are only likely in the vicinity of emission sources or in emission plumes (Sorooshian et al., 2008; Ge et al., 2011). Under such conditions, particle neutralization ratios are likely to be high (Sorooshian et al., 2008), and NH_3 and amines compete for particulate H_3O^+ ions, where DMA can displace NH_4^+ in liquid and NH_3 can displace $DMAH^+$ in solid particles. Although laboratory experiments have shown that in the absence of NH_3, DMA could partially displace NH_4^+ from solid ammonium salts including $(NH_4)_2SO_4$ and NH_4NO_3 (Lloyd et al., 2009; Qiu and Zhang, 2012; Chan and Chan, 2012, 2013), this scenario is unlikely under atmospheric conditions with abundant NH_3.

In this study, we used DMA as a proxy for atmospherically relevant R_3N. As different R_3N and their sulfate and oxalate salts possess different hygroscopic and crystallization properties (Qiu and Zhang, 2012; Clegg et al., 2013; Chan and Chan, 2013;

Chu et al., 2015; Sauerwein et al., 2015) which can all influence uptake behavior, the findings here obtained may not be generalizable to all short-chain aliphatic amine compounds. It should also be mentioned that particle size may affect the particle composition as a result of the uptake, as well as the crystallization of the particle. The observed results may be most relevant to aerosols larger than 1 μm, which were found in the atmosphere to have the highest R_3NH/NH_4 ratio (VandenBoer et al., 2011; Youn et al., 2015). To improve our understanding of the mechanisms governing the simultaneous exchange of NH_3 and R_3N between the gas and particle phases, particle size dependence should be investigated in the future.

Acknowledgements

This work was supported by the Research Grants Council of the Hong Kong Special Administrative Region, China (GRF grant no. 600112 and 16300214).

References

Almeida, J., Schobesberger, S., Kürten, A., Ortega, I. K., Kupiainen-Määttä, O., Praplan, A. P., Adamov, A., Amorim, A., Bianchi, F., Breitenlechner, M., David, A., Dommen, J., Donahue, N. M., Downard, A., Dunne, E., Duplissy, J., Ehrhart, S., Flagan, R. C., Franchin, A., Guida, R., Hakala, J., Hansel, A., Heinritzi, M., Henschel, H., Jokinen, T., Junninen, H., Kajos, M., Kangasluoma, J., Keskinen, H., Kupc, A., Kurtén, T., Kvashin, A. N., Laaksonen, A., Lehtipalo, K., Leiminger, M., Leppä, J., Loukonen, V., Makhmutov, V., Mathot, S., McGrath, M. J., Nieminen, T., Olenius, T., Onnela, A., Petäjä, T., Riccobono, F., Riipinen, I., Rissanen, M., Rondo, L., Ruuskanen, T., Santos, F. D., Sarnela, N., Schallhart, S., Schnitzhofer, R., Seinfeld, J. H., Simon, M., Sipilä, M., Stozhkov, Y., Stratmann, F., Tomé, A., Tröstl, J., Tsagkogeorgas, G., Vaattovaara, P., Viisanen, Y., Virtanen, A., Vrtala, A., Wagner, P. E., Weingartner, E., Wex, H., Williamson, C., Wimmer, D., Ye, P., Yli-Juuti, T., Carslaw, K. S., Kulmala, M., Curtius, J., Baltensperger, U., Worsnop, D. R., Vehkamäki, H., and Kirkby, J.: Molecular understanding of sulphuric acid-amine particle nucleation in the atmosphere, Nature, 502, 359–363, 2013.

Angelino, S., Suess, D. T., and Prather, K. A.: Formation of Aerosol Particles from Reactions of Secondary and Tertiary Alkylamines: Characterization by Aerosol Time-of-Flight Mass Spectrometry, Environ. Sci. Technol., 35, 3130–3138, 2001.

Behera, S. N., Sharma, M., Aneja, V. P., and Balasubramanian, R.: Ammonia in the atmosphere: a review on emission sources, atmospheric chemistry and deposition on terrestrial bodies, Environ. Sci. Pollut. Res., 20, 8092–8131, 2013.

Blake, A. J. and Clegg, W.: Crystal structure analysis: Principles and practice; edited by William Clegg, 2nd ed., International Union of Crystallography book series, 13, Oxford University Press, Oxford, 2009.

Bonner, O. D.: Osmotic and activity coefficients of methyl-substituted ammonium nitrates at 298.15 K, J. Chem. Eng. Data, 26, 148–149, 1981.

Brauman, J. I., Riveros, J. M., and Blair, L. K.: Gas-phase basicities of amines, J. Am. Chem. Soc., 93, 3914–3916, 1971.

Breitmaier, E. and Jung, G.: Organische Chemie: Grundlagen, Stoffklassen, Reaktionen, Konzepte, Molekülstrukturen; 129 Tabellen, 5., überarb. Aufl., Thieme, Stuttgart, New York, XVIII, 1000 S., 2005.

Bzdek, B. R., Ridge, D. P., and Johnston, M. V.: Amine exchange into ammonium bisulfate and ammonium nitrate nuclei, Atmos. Chem. Phys., 10, 3495–3503, 2010a.

Bzdek, B. R., Ridge, D. P., and Johnston, M. V.: Size-dependent reactions of ammonium bisulfate clusters with dimethylamine, J. Phys. Chem. A, 114, 11638–11644, 2010b.

Bzdek, B. R., Ridge, D. P., and Johnston, M. V.: Amine reactivity with charged sulfuric acid clusters, Atmos. Chem. Phys., 11, 8735–8743, 2011.

Chan, L. P. and Chan, C. K.: Displacement of Ammonium from Aerosol Particles by Uptake of Triethylamine, Aerosol Sci.

Tech., 46, 236–247, 2012.

Chan, L. P. and Chan, C. K.: Role of the aerosol phase state in ammonia/amines exchange reactions, Environ. Sci. Technol., 47, 5755–5762, 2013.

Chu, Y., Sauerwein, M., and Chan, C. K.: Hygroscopic and phase transition properties of alkyl aminium sulfates at low relative humidities, Phys. Chem. Chem. Phys., 17, 19789–19796, 2015.

Clegg, S. L., Brimblecombe, P., and Wexler, A. S.: Thermodynamic Model of the System H^+ −NH_4^+ −SO_4^{2-} −NO_3^- −H_2O at Tropospheric Temperatures, J. Phys. Chem. A, 102, 2137–2154, 1998.

Clegg, S. L., Qiu, C., and Zhang, R.: The deliquescence behaviour, solubilities, and densities of aqueous solutions of five methyl- and ethyl-aminium sulphate salts, Atmos. Environ., 73, 145–158, 2013.

Colberg, C. A., Krieger, U. K., and Peter, T.: Morphological Investigations of Single Levitated H_2SO_4 /NH_3 /H_2O Aerosol Particles during Deliquescence/Efflorescence Experiments, J. Phys. Chem. A, 108, 2700–2709, 2004.

Daumer, B., Niessner, R., and Klockow, D.: Laboratory studies of the influence of thin organic films on the neutralization reaction of H_2SO_4 aerosol with ammonia, J. Aerosol Sci., 23, 315–325, 1992.

Davidovits, P., Kolb, C. E., Williams, L. R., Jayne, J. T., and Worsnop, D. R.: Mass accommodation and chemical reactions at gas-liquid interfaces, Chem. Rev., 106, 1323–1354, 2006.

Dawson, B. S. W., Irish, D. E., and Toogood, G. E.: Vibrational spectral studies of solutions at elevated temperatures and pressures. 8. A Raman spectral study of ammonium hydrogen sulfate solutions and the hydrogen sulfate-sulfate equilibrium, J. Phys. Chem., 90, 334–341, 1986.

Dawson, M. L., Perraud, V., Gomez, A., Arquero, K. D., Ezell, M. J., and Finlayson-Pitts, B. J.: Measurement of gas-phase ammonia and amines in air by collection onto an ion exchange resin and analysis by ion chromatography, Atmos. Meas. Tech., 7, 2733–2744, 2014.

Decesari, S., Facchini, M. C., Fuzzi, S., and Tagliavini, E.: Characterization of water-soluble organic compounds in atmospheric aerosol: A new approach, J. Geophys. Res., 105, 1481–1489, 2000.

Deegan, R. D., Bakajin, O., Dupont, T. F., Huber, G., Nagel, S. R., and Witten, T. A.: Capillary flow as the cause of ring stains from dried liquid drops, Nature, 389, 827–829, 1997.

Ervens, B., Sorooshian, A., Lim, Y. B., and Turpin, B. J.: Key parameters controlling OH-initiated formation of secondary organic aerosol in the aqueous phase (aqSOA), J. Geophys. Res. Atmos., 119, 3997–4016, 2014.

Ge, X., Wexler, A. S., and Clegg, S. L.: Atmospheric amines – Part I. A review, Atmos. Environ., 45, 524–546, 2011.

Hall, H. K.: Correlation of the Base Strengths of Amines 1, J. Am. Chem. Soc., 79, 5441–5444, 1957.

Hamacher-Barth, E., Leck, C., and Jansson, K.: Size-resolved morphological properties of the high Arctic summer aerosol during ASCOS-2008, Atmos. Chem. Phys., 16, 6577–6593, 2016.

Hansen, M. J., Adamsen, A. P. S., and Feilberg, A.: Recovery of odorants from an olfactometer measured by proton-transfer-reaction mass spectrometry, Sensors, 13, 7860–7871, 2013.

Hanson, D. and Kosciuch, E.: The NH_3 Mass Accommodation Coefficient for Uptake onto Sulfuric Acid Solutions, J. Phys. Chem. A, 107, 2199–2208, 2003.

Healy, R. M., Evans, G. J., Murphy, M., Sierau, B., Arndt, J., McGillicuddy, E., O'Connor, I. P., Sodeau, J. R., and Wenger, J. C.: Single-particle speciation of alkylamines in ambient aerosol at five European sites, Anal. Bioanal. Chem., 407, 5899–5909, 2015.

Hu, Q., Yu, P., Zhu, Y., Li, K., Gao, H., and Yao, X.: Concentration, Size Distribution, and Formation of Trimethylaminium and Dimethylaminium Ions in Atmospheric Particles over Marginal Seas of China*, J. Atmos. Sci., 72, 3487–3498, 2015.

Huntzicker, J. J., Cary, R. A., and Ling, C.-S.: Neutralization of sulfuric acid aerosol by ammonia, Environ. Sci. Technol., 14, 819–824, 1980.

Jen, C. N., McMurry, P. H., and Hanson, D. R.: Stabilization of sulfuric acid dimers by ammonia, methylamine, dimethylamine, and trimethylamine, J. Geophys. Res. Atmos., 119, 7502–7514, 2014.

Kawamura, K. and Ikushima, K.: Seasonal changes in the distribution of dicarboxylic acids in the urban atmosphere, Environ. Sci. Technol., 27, 2227–2235, 1993.

Kolb, C. E., Cox, R. A., Abbatt, J. P. D., Ammann, M., Davis, E. J., Donaldson, D. J., Garrett, B. C., George, C., Griffiths, P. T., Hanson, D. R., Kulmala, M., McFiggans, G., Pöschl, U., Riipinen, I., Rossi, M. J., Rudich, Y., Wagner, P. E., Winkler, P. M., Worsnop, D. R., and O' Dowd, C. D.: An overview of current issues in the uptake of atmospheric trace gases by aerosols and clouds, Atmos. Chem. Phys., 10, 10561–10605, 2010.

Kulmala, M., Kontkanen, J., Junninen, H., Lehtipalo, K., Manninen, H. E., Nieminen, T., Petaja, T., Sipila, M., Schobesberger, S., Rantala, P., Franchin, A., Jokinen, T., Jarvinen, E., Aijala, M., Kangasluoma, J., Hakala, J., Aalto, P. P., Paasonen, P., Mikkila, J., Vanhanen, J., Aalto, J., Hakola, H., Makkonen, U., Ruuskanen, T., Mauldin, R. L. 3., Duplissy, J., Vehkamaki, H., Back, J., Kortelainen, A., Riipinen, I., Kurten, T., Johnston, M. V., Smith, J. N., Ehn, M., Mentel, T. F., Lehtinen, K. E. J., Laaksonen, A., Kerminen, V.-M., and Worsnop, D. R.: Direct observations of atmospheric aerosol nucleation, Science, 339, 943–946, 2013.

Kulmala, M. and Wagner, P. E.: Mass accommodation and uptake coefficients – a quantitative comparison, J. Aerosol Sci., 32, 833–841, 2001.

Kurtén, T., Loukonen, V., Vehkamäki, H., and Kulmala, M.: Amines are likely to enhance neutral and ion-induced sulfuric acid-water nucleation in the atmosphere more effectively than ammonia, Atmos. Chem. Phys., 8, 4095–4103, 2008.

Kürten, A., Bergen, A., Heinritzi, M., Leiminger, M., Lorenz, V., Piel, F., Simon, M., Sitals, R., Wagner, A., and Curtius, J.: Observation of new particle formation and measurement of sulfuric acid, ammonia, amines and highly oxidized molecules using nitrate CI-APi-TOF at a rural site in central Germany, Atmos. Chem. Phys. Discuss., 1–47, 2016.

Lavi, A., Segre, E., Gomez-Hernandez, M., Zhang, R., and Rudich, Y.: Volatility of atmospherically relevant alkylaminium carboxylate salts, J. Phys. Chem. A, 119, 4336–4346, 2015.

Lee, A. K. Y., Ling, T. Y., and Chan, C. K.: Understanding hygroscopic growth and phase transformation of aerosols using single particle Raman spectroscopy in an electrodynamic balance, Faraday Discuss., 137, 245–263, 2008.

Li, Y. J., Liu, P., Gong, Z., Wang, Y., Bateman, A. P., Bergoend, C., Bertram, A. K., and Martin, S. T.: Chemical Reactivity and Liquid/Nonliquid States of Secondary Organic Material, Environ. Sci. Technol., 49, 13264–13274, 2015.

Liggio, J., Li, S.-M., Vlasenko, A., Stroud, C., and Makar, P.: Depression of ammonia uptake to sulfuric acid aerosols by competing uptake of ambient organic gases, Environ. Sci. Technol., 45, 2790–2796, 2011.

Liu, Y., Ma, Q., and He, H.: Heterogeneous uptake of amines by citric acid and humic acid, Environ. Sci. Technol., 46, 11112–11118, 2012.

Lloyd, J. A., Heaton, K. J., and Johnston, M. V.: Reactive uptake of trimethylamine into ammonium nitrate particles, J. Phys. Chem. A, 113, 4840–4843, 2009.

Lund Myhre, C. E., Christensen, D. H., Nicolaisen, F. M., and Nielsen, C. J.: Spectroscopic Study of Aqueous H_2SO_4 at Different Temperatures and Compositions: Variations in Dissociation and Optical Properties, J. Phys. Chem. A,, 107, 1979–1991, 2003.

Ma, Q., He, H., and Liu, C.: Hygroscopic properties of oxalic acid and atmospherically relevant oxalates, Atmos. Environ., 69, 281–288, 2013.

Macaskill, J. B. and Bates, R. G.: Osmotic and activity coefficients of monomethyl-, dimethyl-, and trimethylammonium chlorides at 25°C, J. Solution Chem., 15, 323–330, 1986.

Mäkelä, J. M., Yli-Koivisto, S., Hiltunen, V., Seidl, W., Swietlicki, E., Teinilä, K., Sillanpää, M., Koponen, I. K., Paatero, J., Rosman, K., and Hämeri, K.: Chemical composition of aerosol during particle formation events in boreal forest, Tellus B, 53, 2001.

McMurry, P. H., Takano, H., and Anderson, G. R.: Study of the ammonia (gas)-sulfuric acid (aerosol) reaction rate, Environ. Sci. Technol., 17, 347–352, 1983.

Müller, C., Iinuma, Y., Karstensen, J., van Pinxteren, D., Lehmann, S., Gnauk, T., and Herrmann, H.: Seasonal variation of aliphatic amines in marine sub-micrometer particles at the Cape Verde islands, Atmos. Chem. Phys., 9, 9587–9597, 2009.

Olenius, T., Kupiainen-Maatta, O., Ortega, I. K., Kurtén, T., and Vehkamäki, H.: Free energy barrier in the growth of sulfuric acid-ammonia and sulfuric acid-dimethylamine clusters, J. Chem. Phys., 139, 84312, 2013.

Parrillo, D. J., Gorte, R. J., and Farneth, W. E.: A calorimetric study of simple bases in H-ZSM-5: A comparison with gas-phase and solution-phase acidities, J. Am. Chem. Soc., 115, 12441–12445, 1993.

Peng, C. and Chan, C. K.: The water cycles of water-soluble organic salts of atmospheric importance, Atmos. Environ., 35, 1183–1192, 2001.

Peng, C., Chan, M. N., and Chan, C. K.: The Hygroscopic Properties of Dicarboxylic and Multifunctional Acids: Measurements and UNIFAC Predictions, Environ. Sci. Technol., 35, 4495–4501, 2001.

Pöschl, U., Rudich, Y., and Ammann, M.: Kinetic model framework for aerosol and cloud surface chemistry and gas-particle interactions – Part 1: General equations, parameters, and terminology, Atmos. Chem. Phys., 7, 5989–6023, 2007.

Pratt, K. A., Hatch, L. E., and Prather, K. A.: Seasonal Volatility Dependence of Ambient Particle Phase Amines, Environ. Sci. Technol., 43, 5276–5281, 2009.

Qiu, C., Wang, L., Lal, V., Khalizov, A. F., and Zhang, R.: Heterogeneous reactions of alkylamines with ammonium sulfate and ammonium bisulfate, Environ. Sci. Technol., 45, 4748–4755, 2011.

Qiu, C. and Zhang, R.: Physiochemical properties of alkylaminium sulfates: hygroscopicity, thermostability, and density, Environ. Sci. Technol., 46, 4474–4480, 2012.

Rehbein, P. J. G., Jeong, C.-H., McGuire, M. L., Yao, X., Corbin, J. C., and Evans, G. J.: Cloud and fog processing enhanced gas-to-particle partitioning of trimethylamine, Environ. Sci. Technol., 45, 4346–4352, 2011.

Robacker, D. C. and Bartelt, R. J.: Solid-Phase Microextraction Analysis of Static-Air Emissions of Ammonia, Methylamine, and Putrescine from a Lure for the Mexican Fruit Fly (Anastrephaludens), J. Agric. Food Chem., 44, 3554–3559, 1996.

Rovelli, G., Miles, R. E. H., Reid, J. P., and Clegg, S. L.: Hygroscopic Properties of Aminium Sulphate Aerosols, Atmos. Chem. Phys. Discuss., 1–32, 2016.

Sauerwein, M., Clegg, S. L., and Chan, C. K.: Water Activities and Osmotic Coefficients of Aqueous Solutions of Five Alkylaminium Sulfates and Their Mixtures with H_2SO_4 at 25 °C, Aerosol Sci. Tech., 49, 566–579, 2015.

Schade, G. W. and Crutzen, P. J.: Emission of aliphatic amines from animal husbandry and their reactions: Potential source of N_2O and HCN, J. Atmos. Chem., 22, 319–346, 1995.

Smith, J. N., Barsanti, K. C., Friedli, H. R., Ehn, M., Kulmala, M., Collins, D. R., Scheckman, J. H., Williams, B. J., and McMurry, P. H.: Observations of aminium salts in atmospheric nanoparticles and possible climatic implications, Proc. Natl. Acad. Sci. U.S.A., 107, 6634–6639, 2010.

Smith, J. N., Dunn, M. J., VanReken, T. M., Iida, K., Stolzenburg, M. R., McMurry, P. H., and Huey, L. G.: Chemical composition of atmospheric nanoparticles formed from nucleation in Tecamac, Mexico: Evidence for an important role for organic species in nanoparticle growth, Geophys. Res. Lett., 35, 2008.

Sorooshian, A., Murphy, S. M., Hersey, S., Gates, H., Padro, L. T., Nenes, A., Brechtel, F. J., Jonsson, H., Flagan, R. C., and Seinfeld, J. H.: Comprehensive airborne characterization of aerosol from a major bovine source, Atmos. Chem. Phys., 8, 5489–5520, 2008.

Swartz, E., Shi, Q., Davidovits, P., Jayne, J. T., Worsnop, D. R., and Kolb, C. E.: Uptake of Gas-Phase Ammonia. 2. Uptake by Sulfuric Acid Surfaces, J. Phys. Chem. A, 103, 8824–8833, 1999.

Tao, Y., Ye, X., Jiang, S., Yang, X., Chen, J., Xie, Y., and Wang, R.: Effects of amines on particle growth observed in new

particle formation events, J. Geophys. Res. Atmos., 121, 324–335, 2016.

VandenBoer, T. C., Petroff, A., Markovic, M. Z., and Murphy, J. G.: Size distribution of alkyl amines in continental particulate matter and their online detection in the gas and particle phase, Atmos. Chem. Phys., 11, 4319–4332, 2011.

Wang, L., Lal, V., Khalizov, A. F., and Zhang, R.: Heterogeneous chemistry of alkylamines with sulfuric acid: implications for atmospheric formation of alkylaminium sulfates, Environ. Sci. Technol., 44, 2461–2465, 2010.

Wexler, A. S. and Clegg, S. L.: Atmospheric aerosol models for systems including the ions H^+ NH_4^+ Na^+ SO_4^{2-} NO_3^- Cl^- Br^- and H_2O, J. Geophys. Res., 107, 2002.

Yao, X., Lau, A. P., Fang, M., Chan, C. K., and Hu, M.: Size distributions and formation of ionic species in atmospheric particulate pollutants in Beijing, China: 2—dicarboxylic acids, Atmos. Environ., 37, 3001–3007, 2003.

Yeung, M. C., Lee, A. K. Y., and Chan, C. K.: Phase Transition and Hygroscopic Properties of Internally Mixed Ammonium Sulfate and Adipic Acid (AS-AA) Particles by Optical Microscopic Imaging and Raman Spectroscopy, Aerosol Sci. Tech., 43, 387–399, 2009.

You, Y., Kanawade, V. P., Gouw, J. A. de, Guenther, A. B., Madronich, S., Sierra-Hernández, M. R., Lawler, M., Smith, J. N., Takahama, S., Ruggeri, G., Koss, A., Olson, K., Baumann, K., Weber, R. J., Nenes, A., Guo, H., Edgerton, E. S., Porcelli, L., Brune, W. H., Goldstein, A. H., and Lee, S.-H.: Atmospheric amines and ammonia measured with a chemical ionization mass spectrometer (CIMS), Atmos. Chem. Phys., 14, 12181–12194, 2014.

Youn, J.-S., Crosbie, E., Maudlin, L. C., Wang, Z., and Sorooshian, A.: Dimethylamine as a major alkyl amine species in particles and cloud water: Observations in semi-arid and coastal regions, Atmos. Environ., 122, 250–258, 2015.

Yu, J. Z., Huang, X.-F., Xu, J. H., and Hu, M.: When Aerosol Sulfate Goes Up, So Does Oxalate: Implication for the Formation Mechanisms of Oxalate, Environ. Sci. Technol., 39, 128–133, 2005.

Zheng, J., Ma, Y., Chen, M., Zhang, Q., Wang, L., Khalizov, A. F., Yao, L., Wang, Z., Wang, X., and Chen, L.: Measurement of atmospheric amines and ammonia using the high resolution time-of-flight chemical ionization mass spectrometry, Atmos. Environ., 102, 249–259, 2015.

Atmos. Chem. Phys. Discuss., doi:10.5194/acp-2016-995, 2016
Manuscript under review for journal Atmos. Chem. Phys.
Published: 17 November 2016

Atmospheric Chemistry and Physics Discussions

Table 1: Experimental conditions including relative humidity (RH), gas mixing ratios, the maximum neutralization ratios ($X_{max\ neutral}$) and neutralization ratios of equilibrated particles (X_{equil}), and the neutralization ratios of equilibrated particles exposed to N_2 for about 5 hours (X_{N2}).

Experiment	Particle composition	RH	[DMA]	[NH_3]	Neutralization ratio[a]		
		%	(ppm)		$X_{max\ neutral}$[b]	X_{equil}	X_{N2}
$NH_{3,1.9ppm,10\%}$	$H_2SO_{4\ (aq)}$	10		1.94 ± 0.13			
$NH_{3,1.9ppm,50\%}$	$H_2SO_{4\ (aq)}$	50		1.93 ± 0.12	2.0 ± 0.1	2.0 ± 0.1	
$DMA_{0.15ppm,10\%}$	$H_2SO_{4\ (aq)}$	10	0.16 ± 0.02		1.5 ± 0.1	1.5 ± 0.1	1.2 ± 0.2
$DMA_{0.15ppm,50\%}$	$H_2SO_{4\ (aq)}$	50	0.16 ± 0.02		1.7 ± 0.1	1.7 ± 0.1	1.7 ± 0.2
$DMA_{1ppm,10\%}$	$H_2SO_{4\ (aq)}$	10	1.00 ± 0.11		1.7 ± 0.1	1.5 ± 0.1	1.2 ± 0.1
$DMA_{1ppm,50\%}$	$H_2SO_{4\ (aq)}$	50	1.00 ± 0.11		1.9 ± 0.1	1.9 ± 0.1	1.7 ± 0.1
$0.1_{\ 10\%}$	$H_2SO_{4\ (aq)}$	10	0.14 ± 0.01	1.89 ± 0.04	2.0 ± 0.1	2.0 ± 0.2	2.0 ± 0.4
$0.1_{\ 50\%}$	$H_2SO_{4\ (aq)}$	50	0.14 ± 0.01	1.89 ± 0.04	2.0 ± 0.1	2.0 ± 0.2	1.9 ± 0.1
$0.5_{\ 10\%}$	$H_2SO_{4\ (aq)}$	10	0.89 ± 0.03	1.93 ± 0.13	2.0 ± 0.1	1.9 ± 0.2	1.9 ± 0.2
$0.5_{\ 50\%}$	$H_2SO_{4\ (aq)}$	50	0.89 ± 0.04	1.83 ± 0.04	2.0 ± 0.1	1.8 ± 0.1	1.7 ± 0.2
$ox0.5_{\ 10\%}$	$H_2C_2O_{4\ (s)}$	10	0.89 ± 0.04	1.82 ± 0.03	0.3 ± 0.1	0.3 ± 0.1	
$ox0.5_{\ 70\%}$	$H_2C_2O_{4\ (aq)}$	70	0.96 ± 0.00	1.86 ± 0.01	1.9 ± 0.2	1.9 ± 0.2	

[a] The neutralization ratio is defined as the number of moles of alkaline species over moles of acidic species, $X = (DMAH+NH_4)/SO_4$ or $X = (DMAH+NH_4)/C_2O_4$. [b] For co-uptake experiments $X_{max\ neutral}$ describes the maximum neutralization ratio of particles before reaching equilibrium.

Atmos. Chem. Phys. Discuss., doi:10.5194/acp-2016-995, 2016
Manuscript under review for journal Atmos. Chem. Phys.
Published: 17 November 2016

Atmospheric Chemistry and Physics Discussions

Table 2: Comparison of DMA/NH_3 (gas) molar ratios at different RH and $DMAH/NH_4$ (particle) ratios at different times (t), as well as the displacement percentage (χ) for $DMAH^+$ (10% RH) and NH_4^+ (50% RH) are given.

Experiment	RH	DMA/ NH_3	DMAH/NH_4				Displacement percentage [e]	
	%		$t_{initial}$ [a]	t_{pc} [b]	$t_{neutral}$ [c]	t_{equil} [d]	χ_{DMAH+}	χ_{NH4+}
$0.1_{10\%}$	10	0.07 ± 0.01	0.07 ± 0.01	0.05 ± 0.01	0.03 ± 0.00	0.02 ± 0.00	42%	
$0.1_{50\%}$	50	0.07 ± 0.01	0.08 ± 0.01		0.07 ± 0.01	0.18 ± 0.02		9%
$0.5_{10\%}$	10	0.46 ± 0.04	0.43 ± 0.04	0.27 ± 0.01	0.19 ± 0.01	0.02 ± 0.00	89%	
$0.5_{50\%}$	50	0.49 ± 0.02	0.34 ± 0.02		0.51 ± 0.04	1.77 ± 0.13		50%
$ox0.5_{10\%}$	10	0.49 ± 0.02	0.25 ± 0.03		0.25 ± 0.03	0.17 ± 0.04		
$ox0.5_{10\%}$	70	0.52 ± 0.52	0.34 ± 0.02	0.34 ± 0.02	0.26 ± 0.01	0.09 ± 0.02		

[a] $t_{initial}$ indicates the time of the first measurement (10-15 min); [b] t_{pc} indicates the time when the majority of particles changed from liquid to solid phase, [c] $t_{neutral}$ indicates the time when particles reached (maximum) neutralization, [d] t_{equil} indicates the time when the particle composition reached equilibrium, [e] The displacement percentage χ_{DMAH+} denotes $n$$DMAH^+$ per particle at time t_{pc} over time t_{equil}; χ_{NH4+} denotes $n$$NH_4^+$ per particle at time $t_{neutral}$ over t_{equil};

Atmos. Chem. Phys. Discuss., doi:10.5194/acp-2016-995, 2016
Manuscript under review for journal Atmos. Chem. Phys.
Published: 17 November 2016

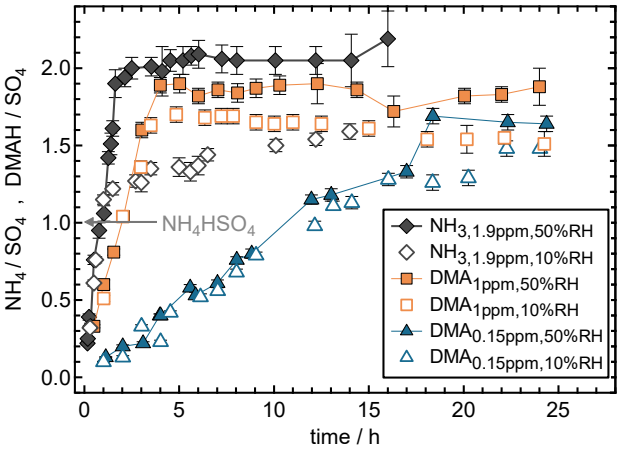

Figure 1: Single gas uptake of NH_3 (1.9 ppm) and DMA (1 ppm and 0.15 ppm) into H_2SO_4, at 10% and 50% RH. NH_4/SO_4 and DMAH/SO_4 denote molar ratios of NH_3 or DMA species to total sulfate species in the particle.

Atmos. Chem. Phys. Discuss., doi:10.5194/acp-2016-995, 2016
Manuscript under review for journal Atmos. Chem. Phys.
Published: 17 November 2016

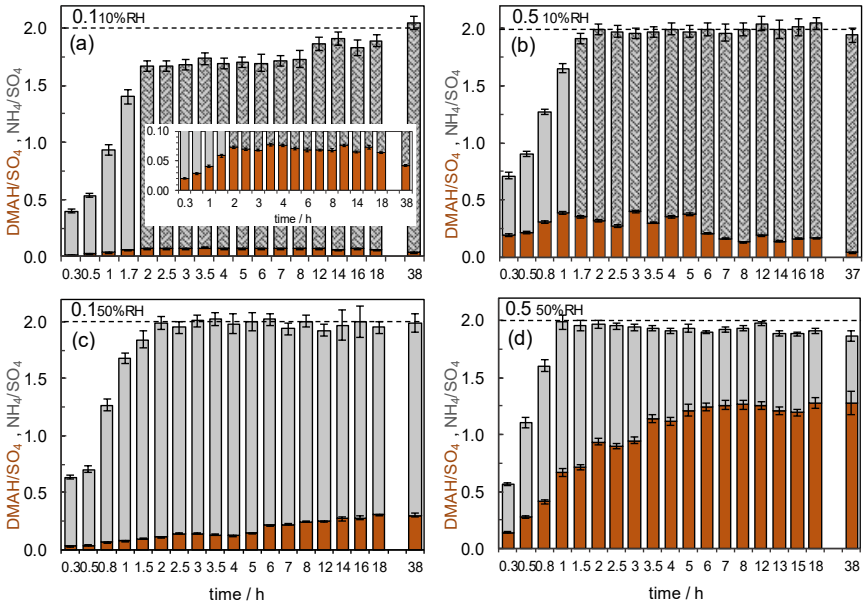

Figure 2: DMA- NH_3 co-uptake of DMA and NH_3 into H_2SO_4 as a function of time: a) DMA/NH_3 = 0.07 at 10% RH ($0.1_{10\%}$), b) DMA/NH_3 = 0.46 at 10% RH ($0.5_{10\%}$), c) DMA/NH_3 = 0.07 at 50% RH ($0.1_{50\%}$), and d) DMA/NH_3 = 0.49 at 50% RH ($0.5_{50\%}$). A value of two indicates complete neutralization of H_2SO_4. Contributions of $DMAH^+$ (brown) and NH_4^+ (grey) to the neutralization are shown as molar ratios (DMAH/SO_4 and NH_4/SO_4). Crosshatched NH_4^+ bars indicate that the majority of particles underwent phase transition from liquid to solid. The inner graph in Fig. 2a is a magnified view of the $DMAH^+$- fraction.

Atmos. Chem. Phys. Discuss., doi:10.5194/acp-2016-995, 2016
Manuscript under review for journal Atmos. Chem. Phys.
Published: 17 November 2016

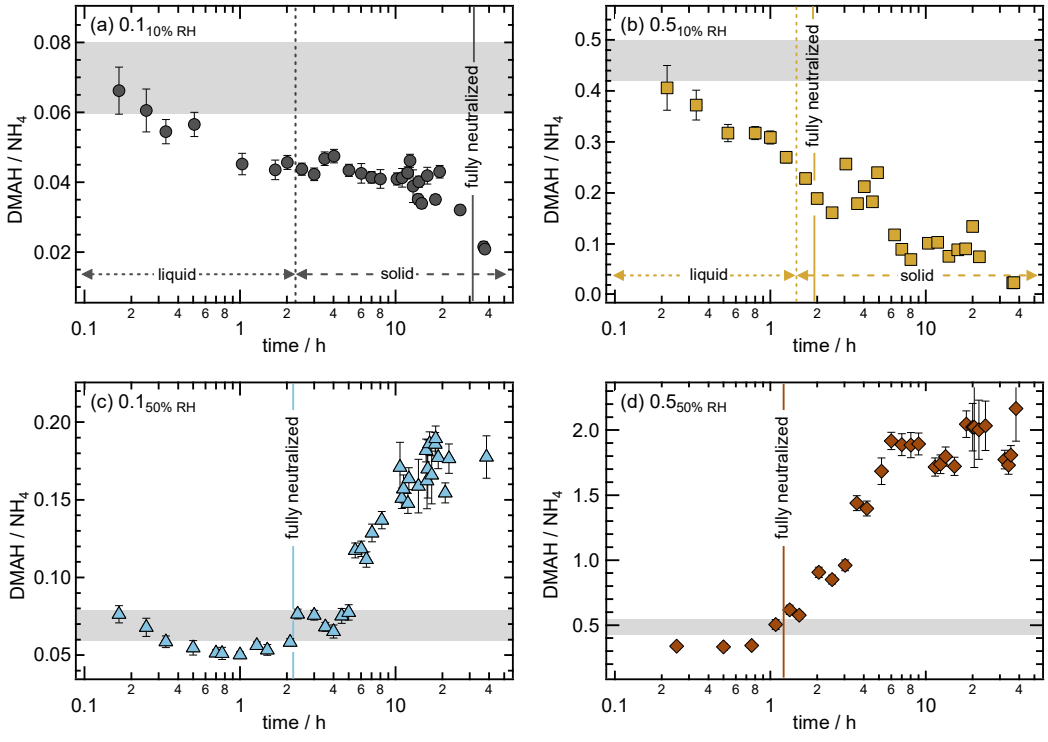

Figure 3: Particulate DMAH/NH_4 molar ratios as a function of time for DMA- NH_3 co-uptake at a) DMA/NH_3 = 0.07 at 10% RH ($0.1_{10\%}$), b) DMA/NH_3 = 0.46 at 10% RH ($0.5_{10\%}$), c) DMA/NH_3 = 0.07 at 50% RH ($0.1_{50\%}$), and d) DMA/NH_3 = 0.49 at 50% RH ($0.5_{50\%}$). DMA/NH_3 gas molar ratios (including uncertainties) are indicated by the grey bands. Dashed vertical lines indicate that the majority of particles underwent phase transition from liquid to solid. Solid vertical lines indicate that particles reached a neutralization ratio of two. Uncertainties from ion chromatography analysis are displayed on the vertical axis unless they are smaller than the symbols.

Atmos. Chem. Phys. Discuss., doi:10.5194/acp-2016-995, 2016
Manuscript under review for journal Atmos. Chem. Phys.
Published: 17 November 2016

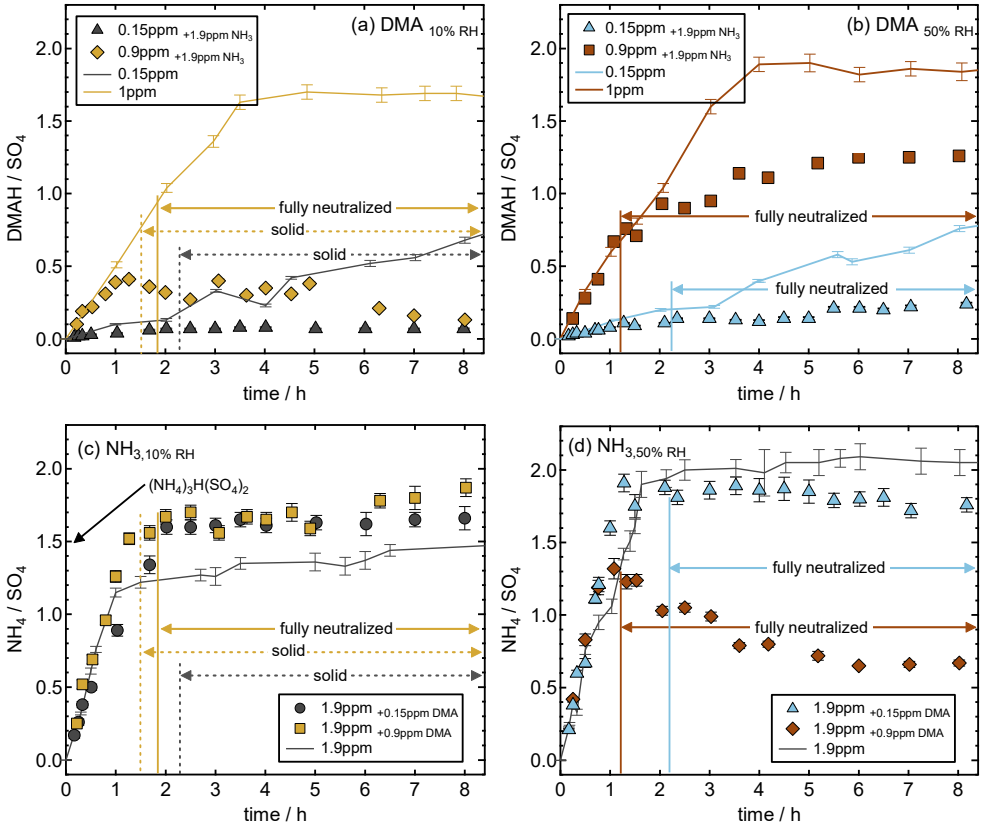

Figure 4: Comparison of particulate DMAH/SO_4 (a, b) and NH_4/SO_4 (c, d) in single gas uptake (line) vs. DMA- NH_3 co-uptake (symbols) into H_2SO_4 at 10% RH (a,c) and 50% RH (b, d), in the first 8 hours of reaction. Dashed vertical lines indicate phase transition of the majority of particles. Solid vertical lines indicate that particles reached a neutralization ratio of two. Uncertainties from ion chromatography analysis are displayed on the vertical axis unless they are smaller than the symbols.

Atmos. Chem. Phys. Discuss., doi:10.5194/acp-2016-995, 2016
Manuscript under review for journal Atmos. Chem. Phys.
Published: 17 November 2016

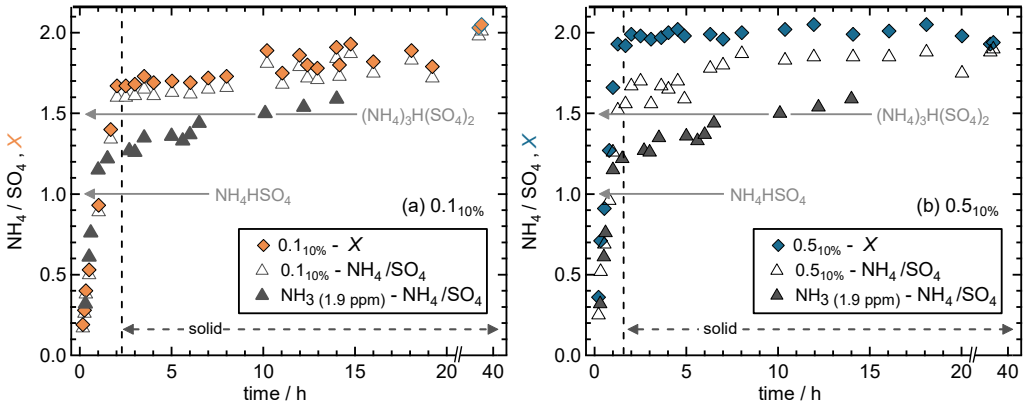

Figure 5: Comparison of particulate NH_4/SO_4 in single gas uptake (filled triangles) vs. DMA- NH_3 co-uptake (open triangles) experiments at 10% RH into H_2SO_4: a) DMA/NH_3 = 0.07, and b) DMA/NH_3 = 0.46. Diamonds denote the net uptake (*X*) in co-uptake experiments. Error bars are omitted for clarity.

Atmos. Chem. Phys. Discuss., doi:10.5194/acp-2016-995, 2016
Manuscript under review for journal Atmos. Chem. Phys.
Published: 17 November 2016

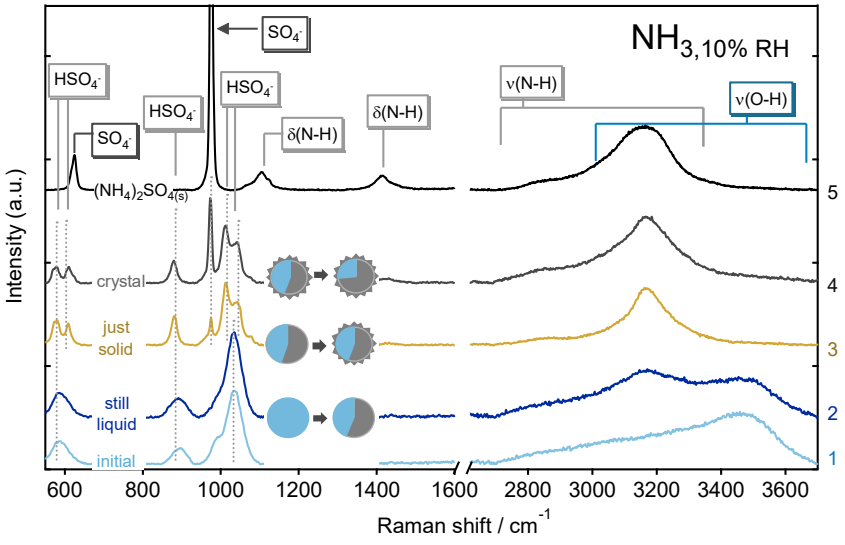

Figure 6: Raman spectra of selected particles representing different phase states during uptake of NH_3 into H_2SO_4 at 10% RH. A spectrum of crystalline $(NH_4)_2SO_4$ is added for reference. Sketches indicate the cation composition range (as inferred from IC measurements) of particles when the spectra were recorded; grey denotes NH_4^+ and blue denotes H_3O^+ (HSO_4^-).

Atmos. Chem. Phys. Discuss., doi:10.5194/acp-2016-995, 2016
Manuscript under review for journal Atmos. Chem. Phys.
Published: 17 November 2016

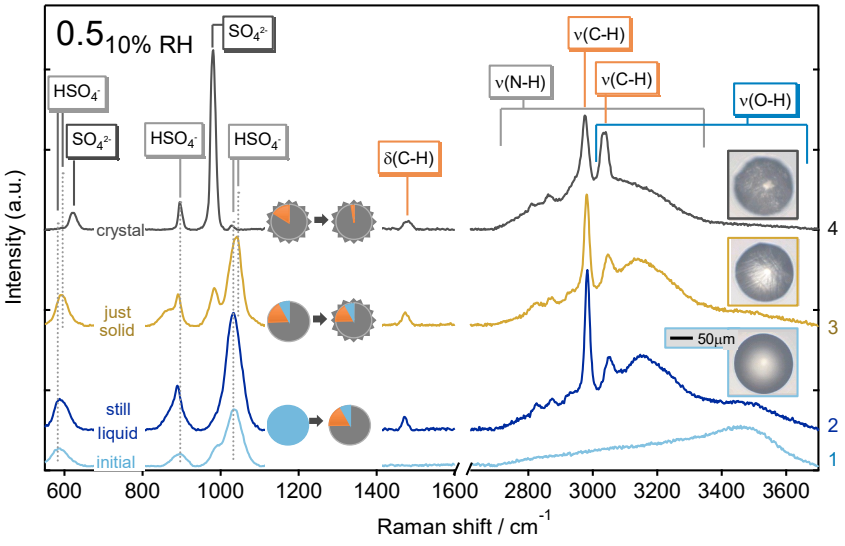

Figure 7: Raman spectra and morphological changes of selected particles during DMA- NH_3 co-uptake into H_2SO_4 at 10% RH at a DMA/NH_3 molar ratio of 0.46 ($0.5_{10\%}$). Sketches indicate the cation composition range (as inferred from IC measurements) of particles when the spectra were recorded. Orange denotes $DMAH^+$, grey denotes NH_4^+, and blue denotes H_3O^+ (HSO_4^-).

Atmos. Chem. Phys. Discuss., doi:10.5194/acp-2016-995, 2016
Manuscript under review for journal Atmos. Chem. Phys.
Published: 17 November 2016

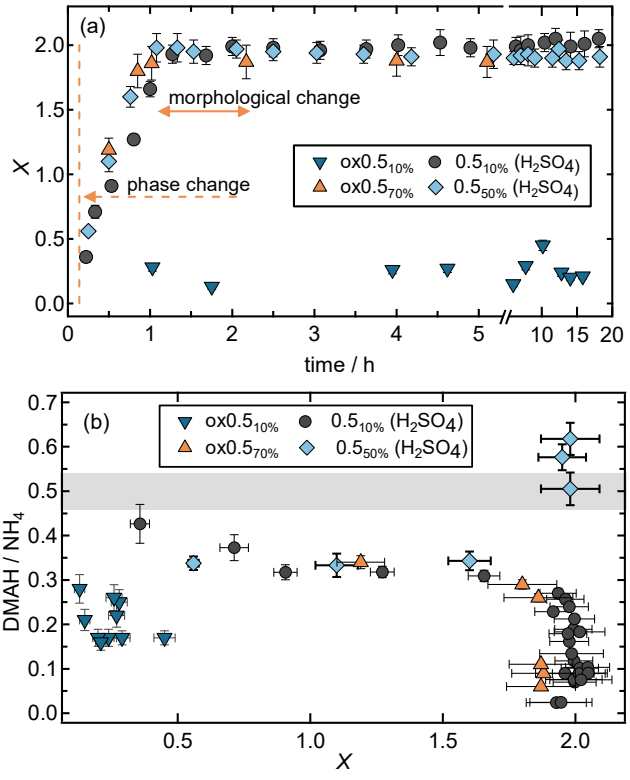

Figure 8: DMA- NH_3 co-uptake at DMA/NH_3 gas molar ratios of 0.5 (given in Table 1) into sulfuric and oxalic acid particles at 10%, 50% and 70% RH. a) Neutralization ratios as a function of time. The vertical dotted line indicates that the majority of oxalic acid particles at 70% RH underwent phase transition from liquid to solid; the vertical solid line indicates the morphological transformation of oxalic acid particles from a non-crystalline to a crystalline morphology at 70% RH. b) DMAH/NH_4 ratios as a function of particle neutralization; the shaded area indicates the gas phase molar ratio of DMA/NH_3 (including uncertainties).

Atmos. Chem. Phys. Discuss., doi:10.5194/acp-2016-995, 2016
Manuscript under review for journal Atmos. Chem. Phys.
Published: 17 November 2016

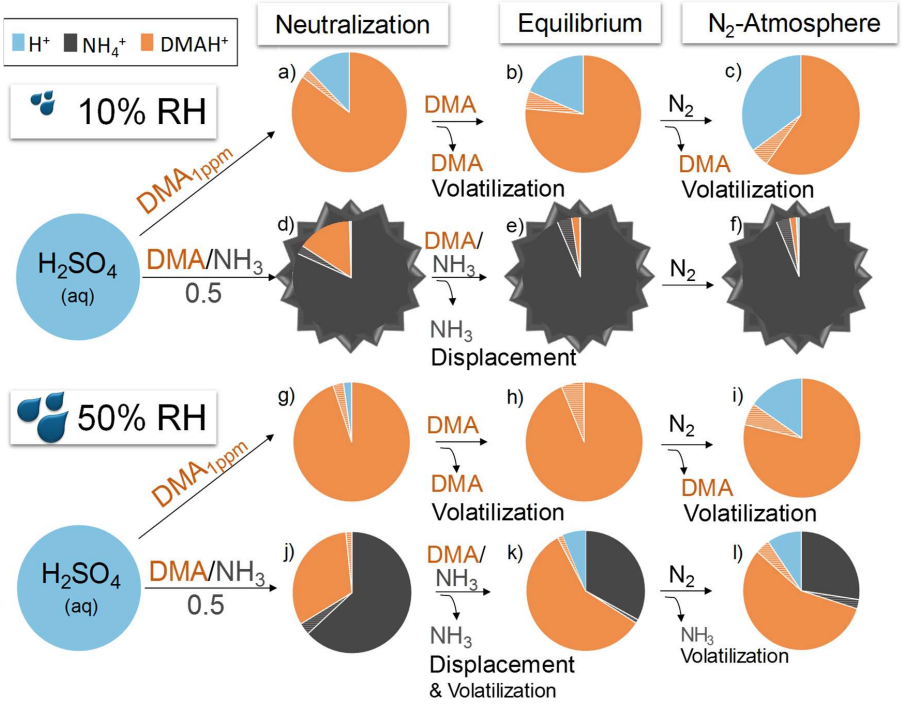

Figure 9: Particle neutralization ratios and the proportion of each cation at maximum neutralization (first column), equilibrium (second column), and after exposure of equilibrated particles to N_2 gas (third column). Color scheme: orange represents $DMAH^+$, grey represents NH_4^+, shaded areas indicate uncertainty of the respective species, and blue represents H_3O^+ (HSO_4^-). Stars around pie charts indicate that particles were crystalline solids. Concentrations of DMA and NH_3 are shown in Table 1.